Dalton Transactions

RSC Publishing

PAPER

View Article Online
View Journal | View Issue

Cite this: *Dalton Trans.*, 2013, **42**, 13576

Synthesis, structural and magnetic characterisation of iron(II/III), cobalt(II) and copper(II) cluster complexes of the polytopic ligand: *N*-(2-pyridyl)-3-carboxy-propanamide†

Mark E. Russell,[a] Chris S. Hawes,[a,b] Alan Ferguson,[a] Matthew I. J. Polson,[a] Nicholas F. Chilton,[b] Boujemaa Moubaraki,[b] Keith S. Murray[b] and Paul E. Kruger*[a]

Received 18th May 2013,
Accepted 9th July 2013

DOI: 10.1039/c3dt51301g

www.rsc.org/dalton

Herein we describe the synthesis, structural and magnetic characterisation of three transition metal cluster complexes that feature the polytopic ligand *N*-(2-pyridyl)-3-carboxypropanamide (**H_2L**): $[Fe_3^{III}Fe_2^{II}(HL)_6(O)(H_2O)_3][ClO_4]_5\cdot 3MeCN\cdot 4H_2O$, **1**, $[Co_8(HL)_8(O)(OH)_4(MeOH)_3(H_2O)]$-$[ClO_4]_3\cdot 5MeOH\cdot 2H_2O$, **2**, and $[Cu_6(L_{ox})_4(MeOH)(H_2O)_3]\cdot MeOH$, **3**. Complex **1** is a mixed valence penta-nuclear iron cluster containing the archetypal $\{Fe_3^{III}O\}$ triangular basic carboxylate cluster at its core, with two Fe(II) ions above and below the core coordinated to three bidentate pyridyl-amide groups. The structure of the octa-nuclear Co(II) complex, **2**, is based upon a central Co_4 square with the remaining four Co(II) centres at the 'wing-tips' of the complex. The cluster core is replete with bridging oxide, hydroxide and carboxylate groups. Cluster **3** contains an oxidised derivative of the ligand, **L_{ox}**, generated *in situ* through hydroxylation of an α-carbon atom. This hexanuclear cluster has a 'barrel-like' core and contains Cu(II) ions in both square planar and square-based pyramidal geometries. Bridging between Cu(II) centres is furnished by alkoxide and carboxylate groups. Magnetic studies on **1–3** reveals dominant antiferro-magnetic interactions for **1** and **2**, leading to small non-zero spin ground states, while **3** shows ferro-magnetic exchange between the Cu(II) centres to give an $S = 3$ spin ground state.

Introduction

The pyridyl, amide and carboxylate functional groups are commonly used ligand donor sets in coordination chemistry as they offer a broad range of potential coordination modes to metal ions from across the periodic table.[1] While the monodentate pyridyl group is limited in the way it might coordinate to a metal ion, the amide and carboxylate functionalities offer a vast array of coordination capacity ranging from mono- and multi-dentate modes to bridging multiple metal ions in the formation of clusters and polymers. Carboxylate ligands have been used as key building blocks in supramolecular chemistry due to the many potential binding modes available to the carboxylate group.[2] These various binding modes are observed often within metallo-clusters that may range in size from two to an impressive eighty-four metal ions.[3] Many of these carboxylate containing cluster-complexes behave as single-molecule magnets (SMMs).[4] In these rapidly evolving areas of research, the search for new polydentate ligands is an ongoing challenge. This has led increasingly to the design of ligands containing multiple functional groups that are capable of binding several metal ions.[5] In this respect, the *N*-(2-pyridyl)-3-carboxypropanamide ligand, **H_2L**, is an excellent candidate for the synthesis of new polynuclear transition metal complexes, Fig. 1.

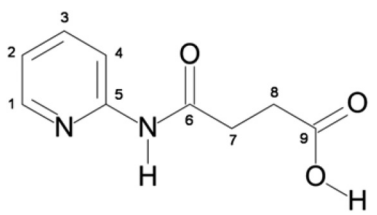

Fig. 1 Structure of the ligand **H_2L** with the labelling scheme used for ^1H and ^{13}C NMR spectroscopy shown.

[a]*MacDiarmid Institute for Advanced Materials and Nanotechnology, Department of Chemistry, University of Canterbury, Private Bag 4800, Christchurch, 8041, New Zealand. E-mail: paul.kruger@canterbury.ac.nz*
[b]*School of Chemistry, Monash University, Clayton, Victoria 3800, Australia. E-mail: keith.murray@monash.edu*

†Electronic supplementary information (ESI) available: ^1H NMR spectrum and single crystal X-ray diffraction data for **H_2L**; hydrogen bonding diagrams and bonding parameters for **H_2L**; magnetisation isotherms for **1–3**. CCDC 939536–939538. For ESI and crystallographic data in CIF or other electronic format see DOI: 10.1039/c3dt51301g

Previous work with $\mathbf{H_2L}$ is limited and has been concerned primarily with its potential biological activity or medicinal application and in the formation of hydrogels.[6] A few studies have reported the spectral characterisation of mononuclear Cu(II) and Ni(II) complexes of $\mathbf{H_2L}$, although no solid-state structures of these species are known.[7] Only one structurally characterised coordination compound has been reported: a discrete mono-nuclear complex, $\{[MnHL(phen)_2]ClO_4{\cdot}1.25H_2O\}$, where $\mathbf{HL^-}$ coordinates *via* a chelating carboxylate group to Mn(II) with 1,10-phenanthroline (phen) present as a co-ligand.[8] Surprised by the dearth of structural reports featuring $\mathbf{H_2L}$, and driven by the recognition of its potentially potent coordination capabilities, we begun an investigation into its coordination chemistry with a variety of 1st row transition metal ions. Here, we report the synthesis and structural characterisation of the first multinuclear cluster complexes of $\mathbf{H_2L}$: a pentanuclear Fe(II/III), an octa-nuclear Co(II) and a hexanuclear Cu(II) species along with details of their magnetic properties.

Experimental

Materials and methods

All reagents were used as received from BDH or Sigma Aldrich. ^{1}H and ^{13}C NMR spectroscopy was carried out on a Varian INOVA 500 spectrometer operating at 500 MHz for ^{1}H and 125 MHz for ^{13}C. High resolution mass spectrometry was recorded on a Bruker maXis 3G UHR-TOF mass spectrometer. Infrared spectra were recorded on a Perkin Elmer Spectrum One FTIR spectrometer in the range 400–4000 cm^{-1}. Samples were analyzed using diffuse reflectance in ground KBr. Elemental analyses (C, H, N) were conducted at Campbell Microanalytical Laboratories, Dunedin.

The magnetic susceptibilities were measured using a Quantum Design Squid magnetometer, MPMS 5, at a dc field of 1 T, with the samples (*ca.* 20 mg) contained in gelatin capsules held at the centre of a drinking straw that was fixed to the end of the sample rod. Ligand diamagnetic corrections were obtained using Pascal's constants. Magnetization isotherms were measured using the same instrument under dc fields of 0 to 5 T at temperatures 2, 3, 4, 5.5, 10, 20 K with samples **1** and **2** dispersed in a Vaseline mull to prevent torquing effects.

The structural analysis at 120 K was performed on an Agilent dual wavelength SuperNova with monochromated Cu-Kα (λ = 1.5418 Å) (**1** and **3**) or Mo-Kα (λ = 0.71073 Å) (**2**) radiation. CrysAlisPro[9] was used for the data collection and data processing. The structure was solved using direct methods with SHELXS[10] and refined on *Olex2*[11] using all data by full matrix least-squares procedures with SHELXL-97.[12] Multi-scan absorption correction using SCALE3 ABSPACK.[13] CCDC numbers: 939536 (**1**); 939537 (**2**); 939538 (**3**).

Synthesis of *N*-(2-pyridyl)-3-carboxypropanamide, $\mathbf{H_2L}$

This synthesis was adapted from the method of Godina and co-workers,[14] full details and spectroscopic data are reported here for the first time. Succinic anhydride (2.73 g, 2.73 × 10^{-2} mol) and 2-aminopyridine (2.57 g, 2.73 × 10^{-2} mol) were dissolved in ethyl acetate (150 ml) and heated at reflux temperature for 24 hours to produce a white solid, which was isolated by filtration, washed with hot ethyl acetate (50 ml) and air dried. Recrystallisation from methanol by slow evaporation afforded colourless needle crystals suitable for a single crystal X-ray diffraction study. Yield 2.08 g, 39%; mp. 180–182 °C (lit. 181–182 °C);[14] HRMS-ESI *m*/*z* (MeOH): Found: 195.0766; $C_9H_{11}N_2O_3$ requires: 195.0764 $[M + H^+]$; δ_H (500 MHz, CD_3OD): 2.66 (2H, t, J = 6.1 Hz, 12.7 Hz, H_8), 2.72 (2H, t, J = 6.1 Hz, 12.7 Hz, H_7), 7.08 (1H, at, J = 6.1 Hz, 1.0 Hz, H_2), 7.74 (1H, at, J = 8.1 Hz, 1.0 Hz, H_3), 8.06 (1H, d, J = 8.1 Hz, H_4), 8.26 (IH, d, J 6.1 Hz, 1.0 Hz, H_1); δ_C (125 MHz, CD_3OD): 28 (C_7), 31 (C_8), 114 (C_4), 119 (C_2), 138 (C_3), 148 (C_1), 152 (C_5), 172 (C_6), 175 (C_9); $\bar{\nu}_{max}$/cm^{-1} (KBr): 3320 br, 3260 br, 3071 m, 2475 m, 1696 s br, 1590 m, 1438 m, 1357 m, 1313 m, 1248 s, 1168 s, 1006 s, 963 m, 916 w, 845 m, 784 s, 745 m, 634 s.

Synthesis and characterisation of the pentanuclear complex: $[Fe_3^{III}Fe_2^{II}(HL)_6(O)(H_2O)_3][ClO_4]_5{\cdot}3MeCN{\cdot}4H_2O$, 1

To a MeCN solution (30 ml) of H_2L (0.13 g, 0.67 mmol) was added $Fe(ClO_4)_2{\cdot}6H_2O$ (0.25 g, 0.67 mmol) followed by the dropwise addition of a 10% Et_3N solution (MeCN, 1 ml). The mixture was stirred for 12 h at 40 °C. Orange plate crystals suitable for a single crystal X-ray diffraction study were isolated after 1 week following the slow evaporation of the reaction mixture. A sample for analysis was dried *in vacuo* overnight to generate the partially desolvated phase of **1** as its monohydrate. Yield: 52 mg, 21%. Found: C, 32.20; H, 3.38; N, 8.08%; $C_{54}H_{60}Cl_5Fe_5N_{12}O_{43}$ requires: C, 32.07; H, 2.99; N 8.32%; $\bar{\nu}_{max}$/cm^{-1} (KBr): 3322 br, 1677 s, 1601 s, 1540 s, 1478 s, 1319 s, 1219 s, 1095 s, 884 m, 788 s, 628 m.

Synthesis and characterisation of the octanuclear complex: $[Co_8(HL)_8(O)(OH)_4(MeOH)_3(H_2O)][ClO_4]_3{\cdot}5MeOH{\cdot}2H_2O$, 2

To a MeOH solution (30 ml) of H_2L (0.13 g, 0.67 mmol) was added $Co(ClO_4)_2{\cdot}6H_2O$ (0.245 g, 0.67 mmol) followed by the dropwise addition of a 10% Et_3N solution (MeOH, 1 ml). Pink block crystals suitable for a single crystal X-ray diffraction study were isolated after 1 week following the slow evaporation of the reaction mixture. A sample for analysis was dried *in vacuo* overnight to generate the desolvated phase of **2**. Yield: 23 mg, 10%. Found: C, 34.50; H, 3.38; N, 9.18%; $C_{72}H_{90}Cl_3Co_8N_{16}O_{45}$ requires: C, 34.89; H, 3.66; N 9.05%; $\bar{\nu}_{max}$/cm^{-1} (KBr): 3318 w br, 1674 s, 1602 m, 1581 m, 1540 s, 1479 s, 1438 s, 1311 s, 1240 m, 1106 s, 783 m, 626 m, 512 m.

Synthesis and characterisation of the hexanuclear complex: $[Cu_6(L_{ox})_4(MeOH)(H_2O)_3]{\cdot}MeOH$, 3

To a MeOH solution (30 ml) of H_2L (0.13 g, 0.67 mmol) was added $Cu(OAc)_2{\cdot}H_2O$ (0.133 g, 0.67 mmol) followed by the dropwise addition of a 10% Et_3N solution (MeOH, 1 ml). Large green block-like crystals suitable for a single crystal X-ray diffraction study were isolated after 2 weeks following the slow evaporation of the reaction mixture. A sample for analysis was dried *in vacuo* overnight to generate the desolvated phase of **3**.

Yield: 16 mg, 11%. Found: C, 33.80; H, 2.97; N, 8.63%; $C_{36}H_{34}Cu_6N_8O_{19}$ requires: C, 34.19; H, 2.71; N 8.87%; $\tilde{\nu}_{max}/cm^{-1}$ (KBr): 3340 w br, 2831 s, 1569 s, 1480 s, 1455 s, 1389 s, 1297 s, 1196 s, 1091 s, 1042 m, 969 s, 916 s, 886 s, 773 s, 746 m, 657 s, 581 m, 527 m.

Results and discussion

The ligand, **H_2L**, was synthesised through the condensation of succinic anhydride with 2-aminopyridine which, following recrystallisation from MeOH, produced colourless crystals. The IR spectrum of **H_2L** displays broad absorbance around 3300 cm^{-1} consistent with the presence of an amide (NH) and a stronger absorbance at around 2475 cm^{-1}, indicating the formation of a hydrogen bond between pyridyl and carboxyl groups. The strong broad peak at 1696 cm^{-1} can be attributed to C═O of free carboxylic groups and C═O of both amide and hydrogen bonded carboxylic acid groups, respectively. These spectroscopic features are consistent with the interactions observed within the solid state structure as determined through X-ray crystallography (ESI†).

Complexes **1–3** were obtained by adding M(II) salts to either MeCN or MeOH solutions of **H_2L** in a 1 : 1 stoichiometry, followed by the addition of Et_3N base, and allowing the resultant solutions to evaporate slowly at ambient temperature. Although isolated with modest yields, multiple crystalline batches were cropped from the mother liquor on further standing. The crystals of **1–3** were of sufficient quality to enable a single crystal X-ray diffraction study to be carried out from which their structures were determined unambiguously.

X-ray crystal structure of 1

The atomic numbering scheme and atom connectivity for **1** are shown in Fig. 2. The structure was refined in the monoclinic $P2_1/c$ space group and crystallographic data are detailed in Table 1. Complex **1** is a pentanuclear mixed valence iron cluster and displays unusual core geometry. Fe(II/III) oxidation states were assigned on the basis of bond valence sum calculations (ESI†), considering the bond lengths and charge balance for the cluster. At the centre of the complex resides the archetypal $\{Fe_3^{III}O\}$ triangular basic carboxylate cluster. The coordination sphere around the Fe(III) ions is comprised of the six carboxylate groups of the ligand tail, which bind in a typical 1,3-bridging mode. The distorted octahedral geometry about each Fe(III) is completed by a central μ_3-oxo-ligand and a coordinated water molecule. This $\{Fe_3O\}$ unit is common in iron-oxo chemistry and has served as a building block for many higher nuclearity clusters.[15] At the periphery of the complex, above and below the triangular cluster, are two Fe(II) centres with pseudo-octahedral geometry. Coordination about these peripheral metal centres is furnished by three pyridyl nitrogen atoms and three amido oxygen atoms from three chelating HL^- ligands to yield an N_3O_3 donor set.

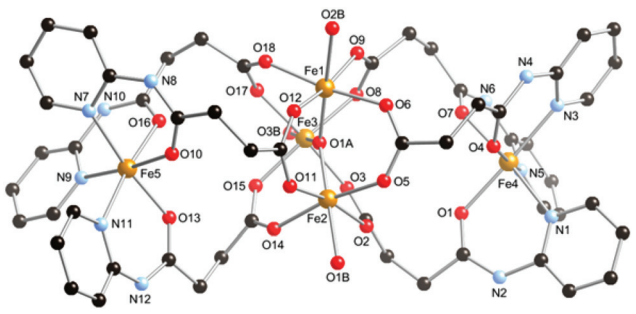

Fig. 2 Molecular structure and atomic labelling scheme for **1**. Hydrogen atoms, perchlorate anions and solvent molecules of crystallisation omitted for clarity.

The separation between the peripheral Fe(II) centres and the central cluster Fe(III) atoms ranges from 5.932(1) to 6.348(1) Å; intra-triangular cluster separations range from 3.269(1) to 3.304(1) Å and the distance between peripheral Fe(II) centres is 11.535 Å through the central cluster. These Fe(II) ions are offset from the centre of the triangular cluster toward the Fe2–Fe3 axis *i.e.* they are not positioned directly above/below the central μ_3-oxo-ligand, O1A. Interestingly, the tris-chelated nature of the HL^- ligands bestows handedness upon the terminal metal ions, which is Δ and Λ about Fe4 and Fe5, respectively. The cluster is therefore a cluster-mesocate; related to the cluster helicates which differ from **1** in that they contain peripheral metal centres that possess the same handedness.[16] To the best of our knowledge this is only the second example of a cluster-mesocate to be structurally characterised.[17]

X-ray crystal structure of 2

The atomic numbering scheme and atom connectivity for **2** are shown in Fig. 3. The structure was refined in the monoclinic $C2/c$ space group and crystallographic data are detailed in Table 1. Compound **2** consists of an octanuclear Co(II) cluster that is built around a $\{Co_4OH\}$ square assembly, with the four remaining Co(II) centres forming the 'wing-tips' of the complex. The Co(II) centres in the $\{Co_4OH\}$ unit (Co2, Co2′, Co3, Co3′) display a distorted octahedral geometry composed of two μ_3-OH (O1H and O2H), one μ_4-OH (O1A) and three carboxylate O atoms (O3, O5 and O11 for Co2; O2, O6 and O8 for Co3). The octahedral geometry of the remaining Co(II) ions (Co1, Co1′, Co4, Co4′) is also distorted. Co4 and Co4′ are bound by one μ_3-OH (O1H), two carboxylate O atoms (O9 and O6), one amido O atom (O4), a pyridyl N atom (N3) and a coordinated MeOH molecule (O14). Co1 and Co1′ also possess a similar donor set: one μ_3-OH (O2H), two carboxylate O atoms (O3 and O12), one amido O atom (O1), a pyridyl N atom (N1); however, the coordinated MeOH molecule (O19) is present with only 25% occupancy with the remaining occupancy filled by a coordinated water molecule.

The HL^- ligand is present in two distinct binding modes. Firstly, in the μ_3:η^2:η^1:η^1:η^1:η^0 mode the ligand chelates to one Co(II) centre at the wing-tip of the complex through the pyridyl N and amido O atoms, while the carboxylate group bridges three Co(II) ions: two from the central core and one from the

Table 1 X-ray crystallography data for **1**, **2** and **3**

	1	2	3
Temperature/K	120(1)	120(1)	120(1)
Chemical formula	$C_{60}H_{77}Cl_5Fe_5N_{15}O_{46}$	$C_{79.5}H_{113}Cl_3Co_8N_{16}O_{52}$	$C_{38}H_{42}Cu_6N_8O_{21}$
Formula mass	2200.82	2702.65	1328.04
Crystal system	Monoclinic	Monoclinic	Monoclinic
a/Å	16.2556(2)	25.9059(4)	41.7229(8)
b/Å	22.8571(4)	14.9866(2)	13.7165(3)
c/Å	25.5874(4)	27.3422(4)	15.3592(3)
α/°	90	90	90
β/°	102.0441(15)	91.2539(15)	91.5503(18)
γ/°	90	90	90
V/Å^3	9297.9(2)	10 612.8(3)	8786.7(3)
Space group	$P2_1/c$	$C2/c$	$C2/c$
Z	4	4	8
λ/Å	1.5418	0.7107	1.5418
μ/mm^{-1}	8.284	1.398	4.009
N_{obs}	56 674	20 971	17 949
N_{unique}	16 567	9391	8599
R_{int}	0.0518	0.0220	0.0283
R_1[a]	0.0998	0.0481	0.0338
wR_2[a]	0.3250	0.1029	0.0940
Goodness of fit	1.195	1.070	1.028

[a] $R_1 = \sum||F_o| - |F_c||/\sum|F_o|$, w$R_2 = [\sum[w(F_o^2 - F_c^2)^2]/\sum[w(F_o^2)^2]]^{1/2}$.

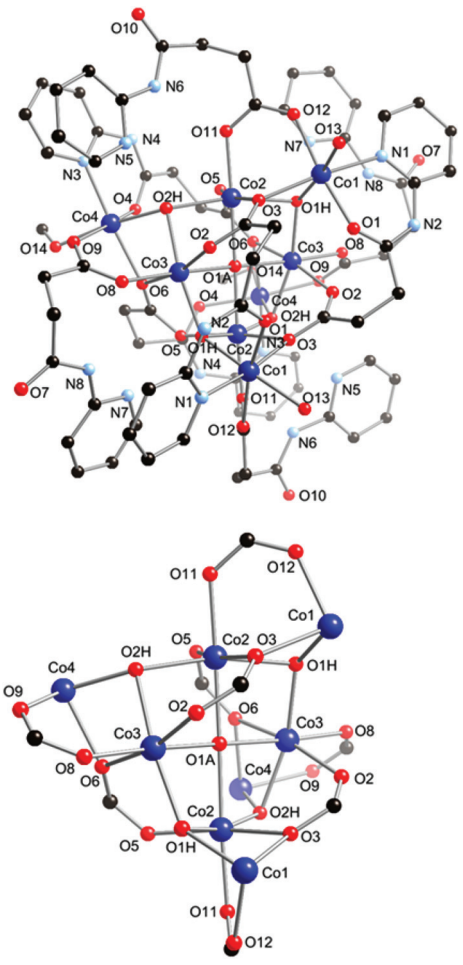

Fig. 3 Molecular structure and partial atom labelling scheme for **2** (top) and the coordination core of **2** showing the potential pathways for magnetic exchange between the Co(II) centres (bottom). Hydrogen atoms and solvent molecules of crystallisation omitted for clarity.

wing-tip. Secondly, the μ_2:η^1:η^1:η^0:η^0:η^0 bonding mode is unbound at the pyridyl end and links a central Co(II) with a wing-tip Co(II) through the 1,3-bridging mode of the carboxylate group. The unbound pyridyl ring is stabilised by both intra- and inter-molecular interactions. Hydrogen bond interactions between the pyridyl nitrogen atom and a μ_3-OH ligand (N5 to O2H and N7 to O1H) and from the adjacent amido NH to a carboxylate O atom (N6 to O11 and N8 to O8) act to stabilise the flexible unbound arm of the ligand. The pyridyl ring is stabilised further by offset intermolecular face-to-face $\pi\cdots\pi$ interaction (N5–C23 to N3–C14 = 3.475(13) Å, N5–C23 to N3″–C14″ = 3.664(14), N7–C32 to N1–C5 = 3.454(13) Å and N7–C32 to N7″–C32″ = 3.452(14) Å).

X-ray crystal structure of 3

The partial atomic numbering scheme and atom connectivity for **3** are shown in Fig. 4. The structure was solved and refined in the monoclinic $C2/c$ space group and the crystallographic data are detailed in Table 1. The data identifies a hexanuclear Cu(II) complex and reveals that an *in situ* oxidation of the ligand has taken place *via* hydroxylation of the α-carbon atom adjacent to the amide carbonyl group, Fig. 4. Hydroxylation of this kind, although not common, is not without precedent and has been shown to proceed through metal directed oxidation involving molecular oxygen.[18] When the reaction was performed under oxygen free conditions, and the solution left to stand under an inert atmosphere in an 'open' vial for several weeks, crystals of **3** failed to form. This is consistent with molecular oxygen being responsible for the hydroxylation, as no precaution was made to exclude water, and is in agreement with the previously proposed mechanism.[18] The resultant ligand is in its triply deprotonated state and the [Cu : L] ratio

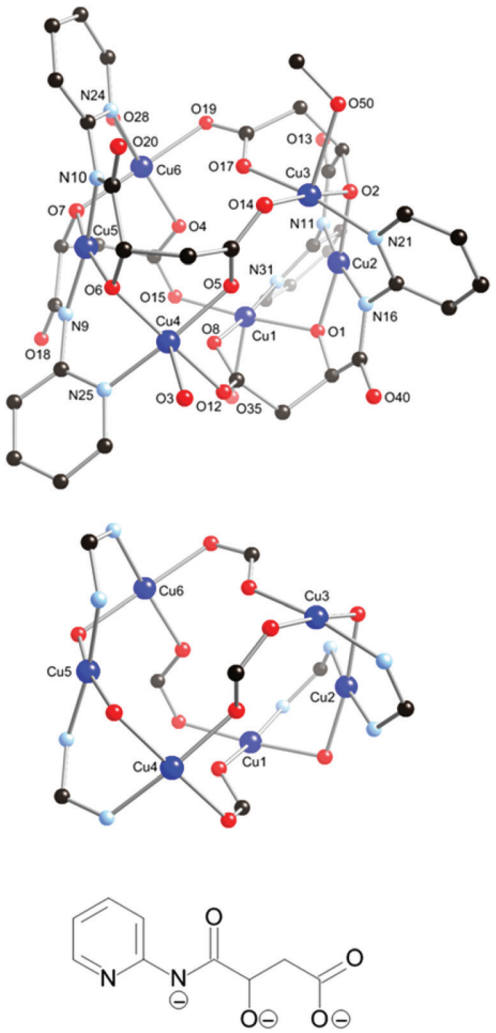

Fig. 4 Molecular structure and partial atomic numbering scheme for **3** (top); the coordination core of **3** showing the potential pathways for magnetic exchange (middle) and the structure of the hydroxylated ligand generated *in situ* (bottom). Hydrogen atoms and solvent of crystallisation removed for clarity.

of 6 : 4 generates a neutral hexanuclear cluster that is best described as having a distorted 'barrel-like' topology.

Two square planar Cu(II) centres (Cu2 and Cu5) reside at the ends of the barrel, while four square-pyramidal Cu(II) ions (Cu1, Cu3, Cu4 and Cu6) occupy its sides. Square planar Cu2 and Cu5 are each bound by two amido nitrogen atoms (N11 and N16 for Cu2; N9 and N10 for Cu5) and two alkoxy oxygen atoms (O1 and O2 for Cu2; O6 and O7 for Cu5) from two different ligands to form two N,O-chelate rings around each Cu centre (four ligands in total). Each of the pyridyl rings adjacent to the coordinated amido groups are rotated by *ca.* 50° to the amido-alkoxy chelate ring plane and coordinate to square-pyramidal Cu(II) ions (Cu1, Cu3, Cu4 and Cu6). The basal plane of the square pyramidal Cu-centres is comprised of a pyridyl nitrogen atom, a bridging alkoxy oxygen atom and two bridging carboxylate oxygen atoms with either a coordinated water molecule (Cu1, Cu4 and Cu6) or methanol molecule (Cu3) located at the apex of the pyramid. The bridging and linking between each Cu-ion in **3** is such that the square or basal planes of the coordination spheres around adjacent Cu-centres subtend angles to each other between *ca.* 98–102° for the twelve angles formed by the six intersecting planes around the barrel.

Each hexanuclear complex is linked to four neighbouring clusters through eight hydrogen bond interactions that involve each amido oxygen atom and the neighbouring coordinated solvent molecules bound to the square-pyramidal Cu(II) ions. These connections create a 2D sheet in the crystallographic *bc* plane. Weak offset face-to-face π···π interactions between each pyridyl ring and its adjacent symmetry related partner (ring centroid–centroid distances range from 3.416(1)–3.763(1) Å) link the cluster to a further three neighbouring clusters along the crystallographic *a*-axis. The shortest intermolecular metal–metal separation is between Cu5 and Cu5′ at 3.683(1).

Magnetic properties

The bulk magnetic properties of **1–3** were probed *via* variable temperature, DC and AC susceptibility measurements on polycrystalline samples. For **1** the $\chi_M T$ value at 300 K is 10.1 cm^3 mol^{-1} K, which is in good agreement with the expected value of ~10.5 cm^3 mol^{-1} K for a basic carboxylate $\{Fe_3O\}$ (S = 5/2 trimer)[19] plus two non-coupled high-spin Fe(II) S = 2 centres, Fig. 5. As the temperature is lowered the $\chi_M T$ product decreases gradually to reach ~7 cm^3 mol^{-1} K at *ca.* 25 K, followed by a more rapid decrease to 1.9 cm^3 mol^{-1} K at 2 K. This behaviour is consistent with dominant antiferromagnetic interactions within the cluster, while the sharp decrease at low temperature is due to zero-field splitting (ZFS).

The magnetization (M) was measured as a function of the applied field at various temperatures (ESI†). It is clear the magnetisation curves are far from saturated. Even at 2 K and 5 T, the M *vs.* H curve is not saturated, but equal to 5.2$N\beta$, consistent with a small non-zero spin ground state for **1**. The general shapes are indicative of antiferromagnetically coupled Fe(III) sites together with the two high-spin Fe(II) sites that have their contributing M values reduced because of spin–orbit coupling and orbital degeneracy effects. Antiferromagnetic coupling in Fe(III)-oxo complexes is common,[20] however, larger complexes containing $\{Fe_3O\}$ building blocks have been shown to display large non-zero spin ground states.[21]

The $\chi_M T$ value of **2** at 300 K is 18 cm^3 mol^{-1} K, which is consistent with eight uncoupled spin-only S = 3/2 Co(II) centres with g = 2.19. The $\chi_M T$ product decreases gradually as the temperature is lowered to reach 0.8 cm^3 mol^{-1} K at 2 K, Fig. 5. This indicates antiferromagnetic exchange coupling between the metal centres. Changing the field in the range 2–70 K gave the same $\chi_M T$ value, thus magnetisable impurities and Zeeman depopulation effects appear to be absent. The magnetisation isotherms were measured using dc fields of 0 to 5 T and temperatures of 2 to 20 K (ESI†). The M values do not saturate and the values at 2 and 3 K at 5 T are similar, 2$N\beta$. These plots suggest the spin ground state is not zero and the low M value at 2 K and 5 T confirms antiferromagnetic coupling probably also influenced by spin–orbit coupling of the parent

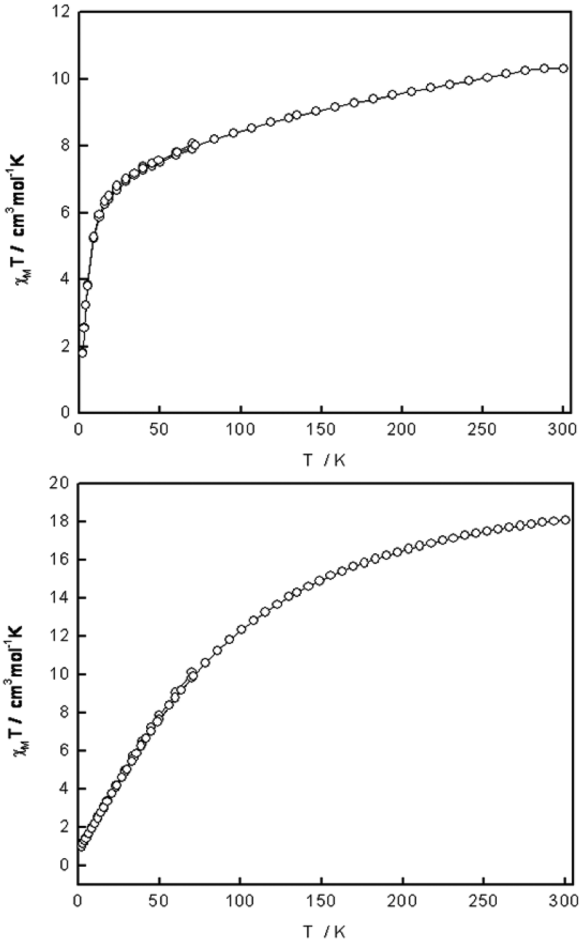

Fig. 5 $\chi_M T$ *vs.* T curves for **1** (top) and **2** (bottom).

$^4T_{1g}$ single-ion states. Measurements of out-of-phase ac susceptibilities, χ''_M, for **2** in the range 2–10 K, gave zero values thus showing that no slow relaxation of magnetisation occurred and no SMM behaviour was observed, as expected for an antiferromagnetically coupled system.

Modelling Co(II) systems in any situation is extremely difficult due to the strong orbital moment and important crystal field effects. This case with eight such octahedral Co(II) ions is at present much too complicated to make any attempt at quantifying the magnetic data. A previously reported Co_8 complex has a similar core to **2**, however, it does not contain a bridging μ_4-OH moiety and the Co(II) ions display trigonal bipyramidal geometry compared to the pseudo octahedral geometry observed in complex **2**.[22] Despite these differences both complexes display similar magnetic behaviour, with antiferromagnetic interactions dominating. Whilst Co(II)-based clusters often display antiferro-magnetic exchange interactions,[23] there are several examples where ferromagnetic interactions lead to the observation of SMM behaviour.[24]

The $\chi_M T$ value of **3** at 300 K is 2.5 cm^3 mol^{-1} K, which is in good agreement with the expected value for six uncoupled S = 1/2 Cu(II) centres with g = 2.10, Fig. 6. As the temperature is decreased towards 50 K, $\chi_M T$ increases gradually to 3.3 cm^3

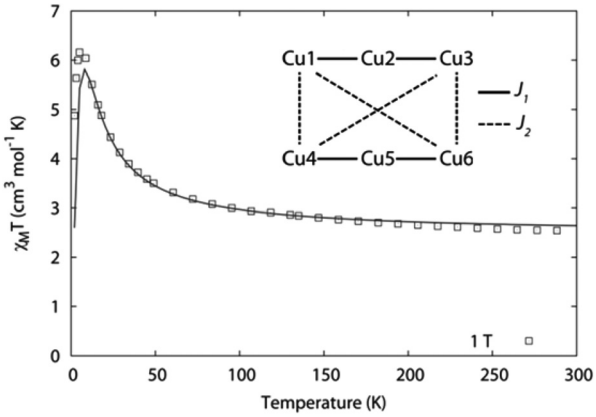

Fig. 6 Fitting of the magnetic data for **3** with *PHI*,[25] using J_1 = 15.1 cm^{-1}, J_2 = 5.18 cm^{-1} and g = 2.10 with proposed coupling scheme (inset).

mol^{-1} K. Then below 50 K there is a more rapid increase in $\chi_M T$ to a maximum of 6.1 cm^3 mol^{-1} K at 4 K, before finally decreasing to 4.9 cm^3 mol^{-1} K at 2 K. Such behaviour is indicative of ferromagnetic exchange coupling with an S = 3 ground spin state. The magnetisation isotherms confirm this behaviour with the 2 K data saturating at $M = 6N\beta$ as expected for an isolated S = 3 ground state (ESI†). Simultaneous fitting of the susceptibility and magnetisation data was performed with the program *PHI*,[25] using the exchange spin Hamiltonian $-2J_1(\hat{S}_1\cdot\hat{S}_2 + \hat{S}_2\cdot\hat{S}_3 + \hat{S}_4\cdot\hat{S}_5 + \hat{S}_5\cdot\hat{S}_6) - 2J_2(\hat{S}_1\cdot\hat{S}_4 + \hat{S}_1\cdot\hat{S}_6 + \hat{S}_3\cdot\hat{S}_4 + \hat{S}_3\cdot\hat{S}_6)$. The J_1 pathways involve {(OR)(1,3-NCN)} bridging while the J_2 pathways involve {*anti*-1,3-OCO} bridging. This two J model reproduced the data extremely well and led to a fit of the magnetic properties giving J_1 = 15.1 cm^{-1}, J_2 = 5.18 cm^{-1} and g = 2.10, Fig. 6. It is more common to observe antiferromagnetic exchange interactions in polynuclear Cu(II) complexes.[26] Complex **3** is one of the few examples of a Cu(II) cluster displaying ferromagnetic interactions, leading to a spin ground state of $S > 1$.[27] Possible reasons for ferromagnetic coupling occurring include the Cu–OR–Cu bridging angles being low, in the range 102–104°, with Cu–Cu separations of ~3.04 Å, and, or combined with, the equatorial planes of individual Cu centres (having Cu($d_{x^2-y^2}$) magnetic orbitals) being orthogonal to those observed for neighbouring centres as one traverses the barrel-shaped cluster; *vide supra* (Fig. 4). The Cu–N–C–N–Cu bridges, from the 2-pyridyl-amido ligand moieties, are not well known for their magnetic exchange features and these might also contribute to ferromagnetic coupling.

Conclusions

This study has identified for the first time some of the potential coordination capability possessed by the polytopic ligand *N*-(2-pyridyl)-3-carboxy-propanamide, **H_2L**. Reaction of **H_2L** with either Fe(II), **1**, Co(II), **2**, or Cu(II), **3**, led to the formation of three new transition metal cluster complexes possessing different and novel core geometries which were structurally and magnetically characterised. Pentanuclear complex **1** and

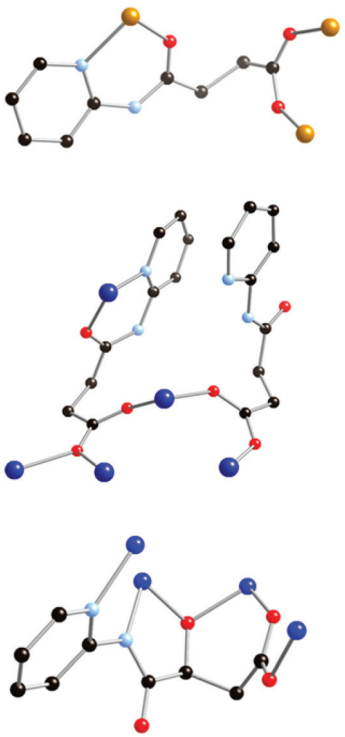

Fig. 7 The different binding modes adopted by the ligands in **1** (top), **2** (middle) and **3** (bottom).

octa-nuclear **2** show dominant antiferromagnetic interaction that leads to small non-zero spin ground states, whereas hexa-nuclear **3** displays ferromagnetic interaction between the Cu(II) centres yielding an $S = 3$ spin ground state. Interestingly, an *in situ* oxidation of $\mathbf{H_2L}$ occurred during the synthesis of **3** *via* the hydroxylation of the α-carbon adjacent to the amide carbonyl group to form $\mathbf{L_{ox}}^{3-}$. $\mathbf{H_2L}$ and its oxidised derivative $\mathbf{H_3L_{ox}}$ are extremely flexible in the nature of their binding to the metal centres, which is highlighted by the presence of four distinct binding modes across the three complexes, Fig. 7. In complexes **1** and **2**, the ligand is mono-deprotonated and binds *via* the pyridyl group and the amido-O atom with the carboxylate group in various bridging modes. However, in complex **3** coordination involves the pyridyl group, and now the amido-N atom (which is deprotonated) and an O-atom from the hydroxyl group in combination with a bridging carboxylate group.

The results presented here suggest that $\mathbf{H_2L}$ has great potential in the synthesis of new polynuclear complexes containing paramagnetic metal ions and we are currently extending this family of complexes to include different metals from across the transition and lanthanide metal ion series and will report upon these examples in the future.

Acknowledgements

The authors thank the University of Canterbury (College of Science Scholarship to CSH), the Royal Society of New Zealand Marsden Fund (PEK), the MacDiarmid Institute for Advanced Materials and Nanotechnology (PEK) and the Australian Research Council (KSM) for financial support. We also thank Dr Anthea Lees (UC) for helpful discussions.

Notes and references

1 W. B. Blanton, S. W. Gordon-Wylie, G. R. Clark, K. D. Jordan, J. T. Wood, U. Geiser and T. J. Collins, *J. Am. Chem. Soc.*, 1999, **121**, 3551–3552; V. Maurizot, G. Linti and I. Huc, *Chem. Commun.*, 2004, 924–925; E. J. L. McInnes, S. Piligkos, G. A. Timco and R. E. P. Winpenny, *Coord. Chem. Rev.*, 2005, **249**, 2577–2590; B. H. Ye, M. L. Tong and X. M. Chen, *Coord. Chem. Rev.*, 2005, **249**, 545–565; C. Kaes, A. Katz and M. W. Hosseini, *Chem. Rev.*, 2000, **100**, 3553–3590; *Terpyridine, Oligopyridine, and Polypyridine Ligands;* R. P. Thummel, in *Comprehensive Coordination Chemistry II*, ed. A. McCleverty and T. J. Meyer, Elsevier, 2003, vol. 1, pp. 41–53; H. W. Roesky and M. Andruh, *Coord. Chem. Rev.*, 2003, **236**, 91–119; H. Hou, Y. Wei, Y. Song, L. Mi, M. Tang, L. Li and Y. Fan, *Angew. Chem., Int. Ed.*, 2005, **44**, 6067–6074; M. Y. Huang, C. Y. Yeh, G. H. Lee and S. M. Peng, *Dalton Trans.*, 2006, 5683–5690; H. Sigel and R. B. Martin, *Chem. Rev.*, 1982, **82**, 385–426; D. J. Tranchemontagne, J. L. Mendoza-Cortes, M. O'Keeffe and O. M. Yaghi, *Chem. Soc. Rev.*, 2009, **38**, 1257–1283.

2 S. R. Batten, S. M. Neville and D. R. Turner, *Coordination Polymers. Design, Analysis and Application*, The Royal Society of Chemistry, 2009; M.-L. Hu, A. Morsali and L. Aboutorabi, *Coord. Chem. Rev.*, 2011, **255**, 2821–2859; C. N. R. Rao, S. Natarajan and R. Vaidhyanathan, *Angew. Chem., Int. Ed.*, 2004, **43**, 1466–1496; E. K. Brechin, C. Boskovic, W. Wernsdorfer, J. Yoo, A. Yamaguchi, E. C. Sañudo, T. R. Concolino, A. L. Rheingold, H. Ishimoto, D. N. Hendrickson and G. Christou, *J. Am. Chem. Soc.*, 2002, **124**, 9710–9711; M. Moragues-Canovás, C. E. Talbot-Eeckelaers, L. Catala, F. Lloret, W. Wernsdorfer, E. K. Brechin and T. Mallah, *Inorg. Chem.*, 2006, **45**, 7038–7040; C. Cañada-Vilalta, T. A. O'Brien, M. Pink, E. R. Davidson and G. Christou, *Inorg. Chem.*, 2003, **42**, 7819–7829; G. Chaboussant, R. Basler, H.-U. Güdel, S. Ochsenbein, A. Parkin, S. Parsons, G. Rajaraman, A. Sieber, A. A. Smith, G. A. Timco and R. E. P. Winpenny, *Dalton Trans.*, 2004, 2758–2766.

3 B. N. Figgis and R. L. Martin, *J. Chem. Soc.*, 1956, 3837; A. J. Tasiopoulos, A. Vinslava, W. Wernsdorfer, K. A. Abboud and G. Christou, *Angew. Chem., Int. Ed.*, 2004, **43**, 2117–2121.

4 R. Sessoli, D. Gatteschi, A. Caneschi and M. A. Novak, *Nature*, 1993, **365**, 141; L. F. Jones, E. K. Brechin, D. Collison, M. Helliwell, T. Mallah, S. Piligkos, G. Rajaraman and W. Wernsdorfer, *Inorg. Chem.*, 2003, **42**, 6601–6603; E. K. Brechin, *Chem. Commun.*, 2005, 5141–5153; R. Bagai and G. Christou, *Chem. Soc. Rev.*, 2009, **38**,

1011–1026; G. E. Kostakis, A. M. Ako and A. K. Powell, *Chem. Soc. Rev.*, 2010, **39**, 2238–2271.

5 Y. S. Moroz, S. Demeshko, M. Haukka, A. Mokhir, U. Mitra, M. Stocker, P. Müller, F. Meyer and I. O. Fritsky, *Inorg. Chem.*, 2012, **51**, 7445–7447; H. Tian, L. Zhao, Y. N. Guo, Y. Guo, J. Tang and Z. Liub, *Chem. Commun.*, 2012, **48**, 708–710; M. U. Anwar, L. K. Thompson, L. N. Dawe, F. Habibb and M. Murugesu, *Chem. Commun.*, 2012, **48**, 4576–4578; P. E. Kruger, B. Moubaraki, G. D. Fallon and K. S. Murray, *J. Chem. Soc., Dalton Trans.*, 2000, 713–718; P. E. Kruger, B. Moubaraki, K. S. Murray and E. R. T. Tiekink, *J. Chem. Soc., Dalton Trans.*, 1994, 2129–2134; D. Pelleteret, R. Clérac, C. Mathonière, E. Harté, W. Schmitt and P. E. Kruger, *Chem. Commun.*, 2009, 221–223; R. J. Archer, C. S. Hawes, G. N. L. Jameson, V. McKee, B. Moubaraki, N. F. Chilton, K. S. Murray, W. Schmitt and P. E. Kruger, *Dalton Trans.*, 2011, **40**, 12368–12373; J. Carranza, H. Grove, J. Sletten, F. Lloret, M. Julve, P. E. Kruger, C. Eller and D. P. Rillema, *Eur. J. Inorg. Chem.*, 2004, 4836–4848; N. R. Kelly, S. Goetz, S. R. Batten and P. E. Kruger, *CrystEngComm*, 2008, **10**, 68–78.

6 A. Nisonoff and D. Pressman, *J. Am. Chem. Soc.*, 1957, **79**, 5565–5572; M. Habash and M. O. Taha, *Bioorg. Med. Chem.*, 2011, **19**, 4746–4771; J. Wu, L. Tang, K. Chen, L. Yan, F. Li and Y. Wang, *J. Colloid Interface Sci.*, 2007, **307**, 280–287; Y. J. Wang, L. Yan, L. M. Tang and J. Yu, *Chin. Chem. Lett.*, 2007, **18**, 1009–1012.

7 B. S. Garg, V. Kumar and M. J. Reddy, *Transition Met. Chem.*, 1993, **18**, 364–368; B. S. Garg, M. J. Reddy and V. Kumar, *J. Coord. Chem.*, 1993, **29**, 33–43; B. S. Garg, V. Kumar and M. J. Reddy, *Indian J. Chem., Sect. A: Inorg., Bio-inorg., Phys., Theor. Anal. Chem.*, 1993, **32**, 726–729; B. S. Garg, V. Kumar and M. J. Reddy, *Indian J. Chem., Sect. A: Inorg., Bio-inorg., Phys., Theor. Anal. Chem.*, 1996, **35**, 598–600.

8 X. Shen, B. Kang, Y. Tong, X. Shi, Y. Li and X. Huang, *J. Coord. Chem.*, 1998, **46**, 105–114.

9 *CrysAlisPro*, Agilent Technologies, Version 1.171.35.19.

10 G. M. Sheldrick, *Acta Crystallogr., Sect. A: Fundam. Crystallogr.*, 1990, **46**, 467.

11 O. V. Dolomanov, L. J. Bourhis, R. J. Gildea, J. A. K. Howard and H. Puschmann, *J. Appl. Crystallogr.*, 2009, **42**, 339.

12 G. M. Sheldrick, *Acta Crystallogr.*, 2008, **A64**, 112–122.

13 *CrysAlisPro*, Agilent Technologies, Version 1.171.35.19; Empirical absorption correction using spherical harmonics, implemented in SCALE3 ABSPACK scaling algorithm.

14 N. V. Kolotova, A. V. Dolzhenko, V. O. Koz'minykh, V. P. Kotegov and A. T. Godina, *Pharm. Chem. J.*, 1999, **33**, 635–637.

15 L. F. Jones, A. Batsanov, E. K. Brechin, D. Collison, M. Helliwell, T. Mallah, E. J. L. McInnes and S. Piligkos, *Angew. Chem., Int. Ed.*, 2002, **41**, 4318–4321; A. Ferguson, J. McGregor, A. Parkin and M. Murrie, *Dalton Trans.*, 2008, 731–733.

16 R. W. Saalfrank, N. Löw, S. Trummer, G. M. Sheldrick, M. Teichert and D. Stalke, *Eur. J. Inorg. Chem.*, 1998, 559–563; R. Ishikawa, M. Nakano, A. Fuyuhiro, T. Takeuchi, S. Kimura, T. Kashiwagi, M. Hagiwara, K. Kindo, S. Kaizaki and S. Kawata, *Chem.–Eur. J.*, 2010, **16**, 11139–11144; S. Romain, J. Rich, C. Sens, T. Stoll, J. Benet-Buchholz, A. Llobet, M. Rodriguez, I. Romero, R. Clérac, C. Mathonière, C. Duboc, A. Deronzier and M. N. Collomb, *Inorg. Chem.*, 2011, **50**, 8427–8436.

17 X. Bao, W. Liu, J. L. Liu, S. Gómez-Coca, E. Ruiz and M. L. Tong, *Inorg. Chem.*, 2013, **52**, 1099–1107.

18 E. Amadei, E. H. Alilou, F. Eydoux, M. Pierrot, M. Reglier and B. Waegell, *J. Chem. Soc., Chem. Commun.*, 1992, 1782–1784; S. Itoh, H. Nakao, L. M. Berreau, T. Kondo, M. Komatsu and S. Fukuzumi, *J. Am. Chem. Soc.*, 1998, **120**, 2890–2899.

19 F. E. Mabbs and D. J. Machin, *Magnetism and Transition Metal Complexes*, Chapman and Hall, 1973, 196–199.

20 S. Koizumi, M. Nihei, M. Nakano and H. Oshio, *Inorg. Chem.*, 2005, **44**, 1208–1210; K. Graham, F. J. Douglas, J. S. Mathieson, S. A. Moggach, J. Schnack and M. Murrie, *Dalton Trans.*, 2011, **40**, 12271–12276.

21 C. Benelli, J. Cano, Y. Journaux, R. Sessoli, G. A. Solan and R. E. P. Winpenny, *Inorg. Chem.*, 2001, **40**, 188–189; C. Cañada-Vilalta, T. A. O'Brien, M. Pink, E. R. Davidson and G. Christou, *Inorg. Chem.*, 2004, **43**, 5505–5521.

22 S. Akine, W. Dong and T. Nabeshima, *Inorg. Chem.*, 2006, **45**, 4677–4684.

23 G. E. Kostakis, S. P. Perlepes, V. A. Blatov, D. M. Proserpio and A. K. Powell, *Coord. Chem. Rev.*, 2012, **256**, 1246–1278.

24 M. Murrie, *Chem. Soc. Rev.*, 2010, **39**, 1986–1995.

25 N. F. Chilton, R. P. Anderson, L. D. Turner, A. Soncini and K. S. Murray, *J. Comput. Chem.*, 2013, **34**, 1164–1175.

26 L. Y. Wang, S. Igarashi, Y. Yukawa, Y. Hoshino, O. Roubeau, G. Aromí and R. E. P. Winpenny, *Dalton Trans.*, 2003, 2318–2324.

27 J. A. Real, G. De Munno, R. Chiappetta, M. Julve, F. Lloret, Y. Journaux, J. C. Colin and G. Blondin, *Angew. Chem., Int. Ed. Engl.*, 1994, **33**, 1184–1186; L. Zhao, Z. Xu, L. K. Thompson, S. L. Heath, D. O. Miller and M. Ohba, *Angew. Chem., Int. Ed.*, 2000, **39**, 3114–3117; P. E. Kruger, G. D. Fallon:, B. Moubaraki, K. J. Berry and K. S. Murray, *Inorg. Chem.*, 1995, **34**, 4808–4814; R. P. Doyle, M. Julve, F. Lloret, M. Nieuwenhuyzen and P. E. Kruger, *Dalton Trans.*, 2006, 2081–2088; X. Zhang, B. Li, J. Tang, J. Tian, G. Huang and J. Zhang, *Dalton Trans.*, 2013, **42**, 3308–3317; L. Merz and W. Haase, *J. Chem. Soc., Dalton Trans.*, 1980, 875–879; C. J. Calzado, *Chem.–Eur. J.*, 2013, **19**, 1254–1261.